In-situ local environment and partitioning of Ni^{2+} ions during crystallization of an oxyfluoride glass

B. Cochain[1,,**], L. Cormier[1], A. Novikova[1], G. Lelong[1], S. Belin[2], X.H. Zhang[3]*

[1]Institut de Minéralogie, de Physique des Matériaux, et de Cosmochimie (IMPMC), Sorbonne Universités - UPMC Univ Paris 06, UMR CNRS 7590, Muséum National d'Histoire Naturelle, IRD UMR 206, F-75005 Paris, France.

[2]Synchrotron SOLEIL, L'Orme des Merisiers, Saint Aubin, France

[3]Laboratoire Verres et Céramique, Université de Rennes 1, UMR CNRS 6226, 35042 Rennes Cedex, France

Abstract

The local structure of Ni^{2+} ions during crystallization of an oxyfluoride aluminosilicate glass was examined by high temperature *in situ* spectroscopic experiments coupled with *in situ* X-ray diffraction to characterize the different crystallization steps. We show that Ni^{2+} ions in the glass are located in the silicate glass network. After heat treatment Ni^{2+} ions do not partition into the fluorine crystallites as observed for rare-earth metals. Instead, we observed the crystallization of a $NiAl_2O_4$ crystalline phase, a largely inverse spinel. The *in situ* spectroscopic results (XRD, UV-Vis-NIR and Ni K-edge XANES) give new insights on the nickel partitioning between the supercooled liquid and the new crystals and show that the inversion degree of $NiAl_2O_4$ spinel during its crystallization depends not only on the temperature but also on the annealing timescale. We also show that the addition of fluorine into aluminosilicate systems favors the formation of spinel crystals at lower temperature than usually observed, thereby playing a role to promote nucleation.

* benjamin.cochain@upmc.fr

** Present address: Institut des Sciences de la Terre de Paris, UMR 7193, ISTeP de l'Université Pierre et Marie Curie, France.

1. Introduction

Materials doped with luminescent ions can be good candidates for optical applications. In particular, transition metals bearing crystalline materials are considered for near-infrared light sources.[1-5] However, crystalline materials do not have a good forming ability, which is a prerequisite for fiber optics fabrication. Instead, glass can be easily shaped and devitrification allows the elaboration of glass-ceramics, for which ultrabroadband optical amplification can be achieved.[4,5] Thanks to their high degree of transparency, durability and good forming ability, oxide glass-ceramics are attractive candidates, but their fluorescence is limited by multiphonon de-excitations caused by a too high phonon energy. On the other hand, glass-ceramics containing metal fluoride crystals, such as alkaline-earth fluorides or rare-earth fluorides, are considered to be materials with high potential for numerous photonic applications due to their low phonon energies.[6-8] Unfortunately, fluoride glasses prior to their crystallization are corrosive, unstable, and can be difficult to shape into fibers.[7,9] Combining the remarkable optical properties of metal ions confined in fluoride crystalline hosts and the elaboration advantages of oxide glasses, lanthanum doped oxyfluoride glass-ceramics have been the subject of numerous studies in the last decade.[6,7,9-11] In these materials, the active metal ions (mostly rare-earths up to now) are incorporated into the low phonon energy lanthanum-fluoride crystals that form during heat treatment.[7,12-14] Both conversion efficiency and emission intensity of this excellent optical material depend on the structural environment, *i.e*. the bonding character and the local structure (ligands, coordination number, bond distance and bond angle) of the metal elements that are embedded into the fluorine containing microcrystalline phases.[6-15]

As Ni^{2+}-doped crystals have attracted much attention because they possess broadband fluorescence covering the whole 1200–1600 nm telecommunication window,[1-3] we have studied in this paper how the local environment of the active transition metal ion Ni^{2+} evolves

during the crystallization of a lanthanum doped oxyfluoride glass. Because Nickel takes the divalent states in almost all hosts, there is no serious need to control its valence.[9,16,17] However, Ni^{2+} can adopt various coordination numbers in silicate glasses with a wide range of associated colorations: four-fold ($^{[4]}Ni$), five-fold ($^{[5]}Ni$) and six-fold coordinated ($^{[6]}Ni$)[17, 18,19] whereas Ni^{2+} is coordinated by 6 F^- ions in fluoride glasses.[9] It has been shown that, after the crystallization of the glass matrix, the fluorescence of Ni^{2+}-doped crystals inside an oxide silicate glass-ceramic is improved significantly by increasing the proportion of Ni^{2+} in octahedral site.[15,16] The determination and the control of the Ni^{2+} ions bonding character and local structure during crystallization is therefore crucial. For this purpose, we have carried out *in situ* X-ray diffraction (XRD) experiments to determine the crystallization sequence, and *in situ* UV-Vis-NIR absorption spectroscopy and X-ray absorption spectroscopy (XAS) at the Ni K-edge in order to determine the Ni^{2+} local environment in the glass and the glass-ceramics as a function of temperature. The use of *in situ* spectroscopic methods as opposed to *ex situ* was invaluable in determining the time- and temperature- dependences of the crystallization mechanisms as well as the temperature dependence of the Ni ions local structure. As a result, the optical properties of the Ni doped glass ceramics are discussed and described in view of the evolution of the local environment of Ni^{2+} during the crystallisation sequence.

2. Materials and methods

The parent Ni-doped lanthanum-oxyfluoride glass was synthesized by melting the dried chemical grade (Al_2O_3, SiO_2, Na_2CO_3, NiO and LaF_3) at 1200°C for one hour in a Pt crucible in an air furnace to match the molar composition 40 SiO_2 - 30 Al_2O_3 - 18 Na_2O - 12 LaF_3: 1 NiO. The melt was quenched on a copper plate. The glass was then ground and remelted twice to ensure chemical homogeneity. The resulting glass composition was checked using microprobe microanalysis (CAMECA SXfive) at the Camparis Center (Université

Pierre et Marie Curie, Paris, France).

In situ high temperature X-ray diffraction (XRD) was carried out using a diffractometer (PANalycal X'Pert PRO) with nickel-filtered Cu Kα radiation. High temperature experiments were made using an Anton Paar HTK 1200 furnace. Data were acquired on the glass at room temperature and a diffractogram was recorded every 10°C between 650 and 800°C. A heating rate of 0.5 °C.min^{-1} was used between each temperature plateau. X-ray diffractograms were analyzed using X-Pert High Score Plus software to determine the crystalline phases through comparison with the software database.

UV-Vis-NIR spectra were acquired from 2490 nm to 300 nm (4000 to 33300 cm^{-1}) with a 2 nm step using a Perkin Elmer Lambda 1050 spectrometer. *In situ* high-temperature studies were performed using a Linkam TS 1500 heating stage, with samples held between two sapphire windows. The temperature calibration of the heating stage was checked using the melting point of Ag, 961.81°C. *In situ* high temperature UV-Vis-NIR transmission spectroscopy has been enabled by placing the heating stage in the path of the light beam deviated of its original path thanks to a series of mirrors (Fig. 1). The transmission spectra were corrected from black body radiation and furnace emissivity as follow:

$$T = (T_s - T_{0\%})/(T_{100\%} - T_{0\%}) \quad (1)$$

where T_s and $T_{100\%}$ are the transmission spectra measured with and without the sample in the heating stage, respectively. $T_{0\%}$ corresponds to the transmission spectrum while occulting the incident beam in order to obtain the emissivity and black body radiation of both the sample and the furnace assemblage. After an initial heating ramp of 100°C/min up to 700°C, isothermal UV-Vis-NIR spectra were recorded during the crystallization process (i.e. at non equilibrium conditions) within 10 minutes in the range 2940-300 nm at 700, 720, 760 and 780°C, using a heating rate of 0.5°C/min between each temperature plateau. The kinetic of the transformation of the local environment of the Ni ion during crystallization of the glass matrix

was monitored by increasing the temperature at a rate of 100°C/min up to 750°C. At this temperature, UV-Vis-NIR spectra were recorded isothermally in a shorter wavelength range, i.e. between 2490 and 600 nm, in order to decrease the acquisition time and to maximize the number of spectra before the loss of the sample transparency due to crystallization. The present *in situ* conditions implied some drawbacks such as a lower resolution and a decrease of the signal-to-noise ratio.

Diffuse reflectance data were acquired on the glass and on the final glass-ceramics quenched products annealed at 700, 750 and 800°C for 120 min to reach thermodynamic and cyrstallization equilibrium. A diffuse reflectance spectrum was also recorded on a crystalline spinel synthesized by Dugue et al.[19] A powder of $BaSO_4$ was used as a reference sample, after being dried up at 500°C for several hours, in order to avoid the harmonics of water in the near-infrared region. The diffuse reflectance data are plotted using the remission function calculated from the Kubelka–Munk theory,[20] $f(R) = (1R)^2/2R = K/S$, where R is the diffuse reflectance, K the volume absorption coefficient, and S the volume scattering coefficient. This function is a good approximation of the actual absorbance of a light scatterer of infinite thickness.[21] Diffuse reflectance spectra can be compared to transmission spectra provided the absorption is not too intense.[22]

The Ni K-edge XAS spectra were collected on the SAMBA beamline at SOLEIL synchrotron using a Si(111) crystal monochromator. Data were collected both in fluorescence mode with a Vortex Silicon Drift Detector and in transmission mode on polish slabs for the glass and glass-ceramic samples and on powder pellets for the crystalline references. For the *in situ* experiments, the Linkam heating stage was set vertical and oriented at 38° with respect to the incident monochromatic beam, in order to optimize fluorescence detection efficiency. Energy was calibrated by reference to a Ni metallic foil. XANES (X-ray Absorption Near Edge Structure) spectra were recorded in approximately 8 minutes on the parent glass sample

and every 10°C between 650 to 850°C with a heating rate of 0.5°C/min. XANES analysis were conducted using the Athena software based on the IFEFFIT program[23] to determine the structural environment of Ni ions. Averaged XAS spectra were first normalized to the absorption edge height and the background removed using the automatic background subtraction routine AUTOBK implemented in the Athena software.[24] Spectra of crystal references were also recorded to decipher the Ni^{2+} coordination through the analysis of XANES pre-edge intensity.[17,25] After interpolating the background over several eV intervals below and above the pre-edge using an arctan function, the maximum intensity of the pre-edge was derived by fitting a pseudo-Voigt function.

3. Results

3.1 X-Ray diffraction

Figure 2 shows the *in situ* X-ray diffractograms of the bulk glass and the glass-ceramics. Although data were acquired every 10°C from 650°C, only the diffractograms for which new diffraction peaks appear are presented for clarity reasons. The parent glass was XRD amorphous up to 720°C. At this temperature, the first crystalline phase that appears corresponds to LaF_3. At 740°C, a second crystalline phase emerges corresponding to nepheline (Na_2AlSiO_4). These results are consistent with previous investigations of the crystallization sequence in similar glass compositions.[13,26-28] By increasing annealing temperature from 760 to 800°C, the amount of crystalline phases increases, resulting in an intensity increase of the Bragg peaks and/or the apparition of new ones. At 800°C, weak intensity diffraction peaks appear and correspond to a $NiAl_2O_4$ spinel crystalline phase[19].

3.2 UV-Vis-NIR spectroscopy

The *in situ* UV-Vis-NIR absorption spectra of the parent glass and the glass-ceramics

are showed in Fig. 3a. These *in-situ* spectra were recorded successfully without waiting for thermodynamic and crystallization equilibrium because of the loss of transparency of the sample when the crystals grow in size. UV-Vis-NIR spectra can help to determine the coordination of Ni^{2+} ions in glasses which can be fourfold, fivefold and sixfold.[17,29] For the parent glass spectrum, three absorption bands centered around 5900, 11700 and 22900 cm^{-1}, along with the shoulder at 18500 cm^{-1}, are assigned to Ni^{2+} ions in trigonal bipyramid sites ($^{[5]}Ni$).[17] The kink near 15800 cm^{-1} can be assigned to Ni^{2+} ions in a tetrahedral site ($^{[4]}Ni$).[17-19,29] These absorption transitions give an overall asymmetrical band spanning over most of the visible spectrum and confer a brown coloration to the initial glass.[18] The *in situ* spectra show a global broadening and a shift to lower wavenumbers of the absorption bands when the temperature is increased. At 700°C, we observe a decrease of the 22900 cm^{-1} absorption band with a slight increase of the 15800 cm^{-1} band assigned to $^{[4]}Ni$. This latter band also slightly shifts to lower wavenumbers with increasing temperatures. We also observe the appearance of a shoulder at 25500 cm^{-1} attributed to Ni^{2+} ions in octahedral sites ($^{[6]}Ni$).[17,19,30] Between 700°C and 780°C, the changes are more important and simultaneous with the appearance of a broad band at 9000 cm^{-1} attributed to both $^{[4]}Ni$ and $^{[6]}Ni$ contributions.[17,19,30] Between 760 and 780°C, the transmitted intensity of the spectra decreases and the high wavenumber signal saturates because of the loss of the sample transparency due to crystallization.

The UV-Vis-NIR spectra recorded *ex situ* for samples heat treated at 700, 750 and 800°C during 2 hours are presented in Fig. 3b. To emphasize the evolution of the absorption band intensities, all spectra but the one at 700°C have been scaled to the band at 15 500 cm^{-1} of the 750°C spectrum. Similar but more resolved spectral changes are observed: (i) a decrease in intensity of the 22900 cm^{-1} band ($^{[5]}Ni$), and (ii) an increase in intensity of the bands related to $^{[4]}Ni$ (9000 and sharp double absorption band at ~ 17000 cm^{-1}) and $^{[6]}Ni$ (9000 and 25500 cm^{-1}). These changes are progressive between 700 and 800°C. From 750°C,

a new absorption band is visible at 13900 cm^{-1} for the spectra recorded on the annealed samples and can be attributed to $^{[6]}Ni$.[30]

The isothermal kinetic experiment at 750°C (Fig. 3c) reveals that the band characteristic of both $^{[4]}Ni$ and $^{[6]}Ni$ at 9000 cm^{-1} appears after 20 minutes simultaneously with the $^{[4]}Ni$ band at 15800 cm^{-1}.[5,17,19,30] These spectral changes are more pronounced after 40 minutes. Then, after 60 minutes, we notice the appearance and the increase of the 12700 cm^{-1} band ($^{[6]}Ni$).[30]

3.3 Ni K-edge XANES

The *in situ* Ni K-edge XANES spectra at 750, 760 and 800°C are shown in Fig. 4 along with the ones of the $NiAl_2O_4$ reference and the parent glass at room temperature. Up to 750°C, the XANES spectra are identical to that of the parent glass. At 750°C, very slight modifications of the Ni K-edge XANES spectrum are observed: the shape resonance at 8350 eV, corresponding to transitions to bound states close to the continuum (n_p states), shifts towards higher energy and the intensity of the first EXAFS oscillation at 8400 eV slightly increases. These trends are accentuated on the spectra recorded at 760 and 800°C. In addition, a new feature appears at 8365 eV, which is also present in the XANES spectrum of Ni-spinel. The changes in the *in situ* XANES spectra point to a modification of the Ni local environment during the crystallization of the sample.

Fig. 5a shows the evolution of the XANES pre-edge feature as a function of temperature. The pre-edge corresponds to transitions to partly filled 3d levels. In octahedral symmetry, these transitions are dipole-forbidden and are slightly enhanced in non centro-symmetric sites. In tetrahedral symmetry, these transitions are electric dipole allowed and the pre-edge is more intense compared to octahedral symmetry.[31] From the parent glass up to 700°C, no change in the pre-edge feature are observed while, between 700 and 800°C, we

notice a decrease in intensity. Until 720°C, the pre-edge intensity is characteristic of a mixture of $^{[4]}Ni$ and $^{[5]}Ni$ with a majority of $^{[5]}Ni^{2+}$.[17,25] At 720°C the pre-edge intensity decreases progressively until reaching a minimum around 800°C. (Fig. 5b) This intensity decrease is characteristic of an increase of the mean coordination number of the Ni^{2+} ions.[17,25]

4. Discussion

4.1 Ni^{2+} sites in the glass and thermal expansion

As compared to previous studies,[17,25,29] both the UV-ViS-NIR and XAS results are consistent with a mixture of $^{[4]}Ni$ and $^{[5]}Ni$ in the parent glass, with a majority of $^{[5]}Ni$. The major changes observed in the *in situ* UV-Vis-NIR spectra with increasing temperature (Fig. 3a) are due to the modification of the Ni^{2+} environment during the crystallization but also to the thermal site expansion at high temperature. The UV-Vis-NIR spectra at 700°C (Fig 3a) and at 750°C (Fig. 3c) have both been recorded just 1 minute after reaching the plateau temperature, so that the temperature effects on the local Ni^{2+} environment prevail over those of crystallization. The most important modifications of the absorption bands with temperature are a shift towards lower wavenumbers (red shift) and an intensity decrease. The red shift, noticeable by a shift of ~1200 cm^{-1} of the Ni absorption bands between the *ex* and *in situ* results, is directly related to the influence of the thermal site expansion on the crystal field splitting of Ni^{2+} ions and is caused by larger bond lengths. A similar shift has been observed in Cr^{3+} and Fe^{2+} bearing silicate glasses of different compositions.[32,33]

4.2 $NiAl_2O_4$ formation

The similarity of the diffuse reflectance and the XANES spectra of the $NiAl_2O_4$ spinel and that of the glass-ceramic annealed at 800°C (Fig. 3b) leads to conclude to the formation of a $NiAl_2O_4$ spinel phase in the glassy matrix[5,17,19,30]. Though spinel diffraction peaks are not

seen in the XRD signal until the 800°C temperature step, the colour evolution, from brown to green to blue, of the annealed glass-ceramics and the *in situ* optical and XAS spectroscopies indicate a change in the Ni environment at temperature lower than 800°C since these techniques are very sensitive to local structural changes. The UV-Vis-NIR spectra at 700°C show an increase in the intensity of the absorption bands attributed to $^{[6]}$Ni and $^{[4]}$Ni and a decrease in intensity of the band attributed to $^{[5]}$Ni. These coordination changes around Ni are expected for $NiAl_2O_4$ which is an inverse spinel structure where Ni^{2+} ions occupy principally octahedral sites. The changes are less visible for XAS spectra as we have an overlap of all Ni sites: no changes in the XANES spectra are observed between 650 and 700°C (Fig. 4). Contrary to changes observed in the optical spectra, the pre-edge intensity remains constant given the error bars up to 720°C (Fig. 5). This can be due to Ni remaining in majority in $^{[5]}$Ni sites or to an antagonistic effect between $^{[4]}$Ni and $^{[6]}$Ni sites: $^{[4]}$Ni increases the pre-edge intensity while $^{[6]}$Ni decreases it. However, the coloration of the annealed samples that evolves from brown for the glass to dark green at 700°C highlights the newly formed $^{[6]}$Ni sites detected by optical absorption.

Above 720°C, the changes around Ni are obvious in XAS spectra. The pre-edge intensity (Fig. 5b) begins to decrease at 720°C and reaches a constant value at 800°C. This intensity decrease reveals an increasing proportion of $^{[6]}$Ni. This strongly suggests an onset of the crystallization of $NiAl_2O_4$ spinel at 700-720°C and spinel formation at 800°C. Indeed, the pre-edge feature do not show further evolution above 800°C and the absorption band characteristic of $^{[5]}$Ni (22900 cm^{-1}) remains as a shoulder of the $^{[6]}Ni^{2+}$ band at 25500 cm^{-1} in the UV-Vis-NIR spectrum recorded on the annealed sample at 800°C (Fig. 3b). This indicates that the Ni coordination evolution is completed at 800°C, implying that most of Ni^{2+} ions are incorporated within the octahedral and tetrahedral sites of spinel crystals while the residual glass is depleted in Ni^{2+} ions in five-fold coordination.

From a kinetic point of view, the UV-Vis-NIR spectra recorded at 750°C (Fig. 3c) show the intensity increase of the absorption bands attributed to $^{[4]}$Ni and $^{[6]}$Ni. After 40 minutes, these new bands are clearly resolved. Their intensity increase stabilizes after 60 minutes when the band characteristic of $^{[6]}$Ni at 13900 cm^{-1} band becomes apparent. It indicates a particular growth mechanism of the $NiAl_2O_4$ spinel phase at 750°C where, in a first stage, both four- and six-fold coordinated Ni^{2+} ions are formed and, in a second stage, only the amount of $^{[6]}$Ni increases until reaching equilibrium after 100 minutes when the spinel phase is essentially inverse, given rise to the green color of the glass-ceramics product annealed for 120 min at 750°C. Though $NiAl_2O_4$ spinels are largely inverse, Ni^{2+} ions can enter tetrahedral sites to a large proportion with increasing temperature, tending towards a random distribution of Ni and Al cations over tetrahedral and octahedral sites.[34,35] This Ni site redistribution appears at vey low temperature compared to a previous investigation.[19] For instance the 800°C spectrum in Figure 3b is similar to the 1200°C spectrum in Dugue *et al*.[19]with the growth of the sharp double absorption at 17000 cm^{-1} in the ex-situ UV-Vis-NIR spectra due to Ni^{2+} in four-fold coordination. The coloration of the annealed samples evolves also from green to blue between 750 and 800°C highlighting the redistribution of Ni over tetrahedral sites. It is thus possible to obtain a Ni redistribution over octahedral and tetrahedral sites in $NiAl_2O_4$ spinel at lower temperature in the present system.

4.3 Association between LaF_3, nucleation sites and Ni partitioning

The evolution of the Ni^{2+} local environment in the glass and during thermal treatment sheds light on the microscopic mechanisms governing the nickel repartition in oxyfluoride silicate glasses and glass-ceramics. Three different phases crystallize from the parent glass: LaF_3 is the first one to crystallize at 720°C possibly alone or subsequently followed by the spinel $NiAl_2O_4$ crystalline phase, and later by the crystallization of nepheline.[13,27,28] Crystallization

of the low phonon energy LaF_3 phase has been extensively studied in rare-earth oxyfluoride glass-ceramics in which active rare earth ions partition into the LaF_3 crystals, giving rise to desired optical properties.[7,36] The present *in situ* XRD, UV-Vis-NIR and Ni K-edge XANES spectroscopic results indicate an evolution of the nickel coordination in the silicate matrix or within an oxide environment. When crystallization occurs, most of Ni^{2+} ions adopt an environment consistent with that of a Ni-spinel phase. There is no evidence that Ni is surrounded by F^- ligands in the glass or in the newly formed crystals despite that Ni^{2+} ions can occur in octahedral sites with six F^- ions as observed by optical absorption and EXAFS experiments in fluoride glasses.[9] It has been shown that fluorine has a marked preference to form bonds with high field strength modifying cations,[37] which can explain that F atoms would be preferentially associated with La^{3+} ions over Ni^{2+} ions, favouring the formation of LaF_3 crystals. In addition, LaF_3 has been shown to crystallize upon heat-treatment in the $40SiO_2–30Al_2O_3–18Na_2O–12LaF_3$ parent glass from nano-sized phase-separated droplets regions enriched with silicon and lanthanum atoms already present in the glass.[27,28,38] The formation of embryos enriched with La and F and their subsequent growth to LaF_3 nanocrystals suggests that the fluorite structure phase firstly crystallises and could promote the $NiAl_2O_4$ spinel phase. This association could explain the formation of spinel crystals at much lower temperature compared to other aluminosilicate systems.[19] Therefore, the addition of LaF_3 into an aluminosilicate oxide glass does not promote the introduction of Ni^{2+} ions within a fluorine crystalline environment as seen for rare-earth ions, but it seems to favor the formation of spinel crystals at lower temperature than already observed[19].

5. Conclusion

The local structure of Ni^{2+} ions during crystallization of a lanthanum oxyfluoride aluminosilicate glass matrix was examined by *in situ* spectroscopic experiments coupled with

in situ diffraction to follow the crystallization of the sample. We show that Ni^{2+} ions in the glass are located in the silicate glass network and do not partition into the fluorine crystallites as observed for rare-earth metals during crystallisation. Instead, we observed the crystallization of a $NiAl_2O_4$ inverse spinel. However, we show that the addition of LaF_3 into aluminosilicate systems favors the formation of spinel crystals at lower temperature than usually observed. In addition, our *in situ* spectroscopic results show that the inversion degree of $NiAl_2O_4$ spinel during its crystallization depends not only on the temperature but also on the annealing timescale. Therefore, the fluorescence and optical properties of Ni-doped oxyfluoride glass-ceramics, improved by a greater $^{[6]}Ni$ proportion, should be maximized by controlling carefully both the annealing temperature and duration of the heat treatment. An interesting perspective for excellent optical applications would be to study a lanthanum oxyfluoride aluminosilicate doped with both nickel and rare-earth ions where the formation of rare-earth fluorites and six-fold coordinated nickel spinels could be controlled.

Acknowledgments

This work was supported by an ANR grant (project GCWEB). The authors thank M. Fialin, L. Galoisy and C. Point for help with electron microprobe experiments, fruitful discussions and glass synthesis respectively and A. Dugué for valuable advice and help at various stage of this study.

References

[1]P. F. then, A. Mooradian, and T. B. Reed, "Efficient cw optically pumped Ni:MgF_2 laser," Opt. Lett., 3[5] 164-66 (1978).

[2]M. V. Iverson, J. C. Windscheif, and W. A. Sibley, "Optical parameters for the MgO:Ni^{2+} laser system," Appl. Phys. Lett., 36[3] 183-84 (1980).

[3]L. F. Johnson, A. M. Johnson, H. J. Guggenheim, and D. Bahnck, "Phonon-terminated laser emission from Ni^{2+} ions in $KMgF_3$," Opt. Lett., 8[7] 371-73 (1983).

[4]T. Suzuki and Y. Ohishi, "Broadband 1400 nm emission from Ni^{2+} in zinc-alumino-silicate glass," Appl. Phys. Lett., 84[19] 3804-06 (2004).

[5]T. Suzuki, G. S. Murugan, and Y. Ohishi, "Optical properties of transparent Li_2O-Ga_2O_3-SiO_2 glass-ceramics embedding Ni-doped nanocrystals," Appl. Phys. Lett., 86[13] 131903 (2005).

[6]M. Mortier and F. Auzel, "Rare-earth doped transparent glass-ceramics with high cross-sections," J. Non-Cryst. Solids, 256-257 361-65 (1999).

[7]M. J. Dejneka, "The luminescence and structure of novel transparent oxyfluoride glass-ceramics," J. Non-Cryst. Solids, 239 149-55 (1998).

[8]S. Tanabe, H. Hayashi, T. Hanada, and N. Onodera, "Fluorescence properties of Er^{3+} ions in glass ceramics containing LaF_3 nanocrystals," Opt. Mater., 19[3] 343-49 (2002).

[9]H. Shigemura, M. Shojiya, R. Kanno, Y. Kawamoto, K. Kadono, and M. Takahashi, "Optical Property and Local Environment of Ni^{2+} in Fluoride Glasses," J. Phys. Chem. B, 102[11] 1920-25 (1998).

[10]J. Mendez-Ramos, V. Lavin, I. R. Martin, U. R. Rodriguez-Mendoza, J. A. Gonzalez-Almeida, V. D. Rodriguez, A. D. Lozano-Gorrin, and P. Nuñez, "Optical properties of Er^{3+} ions in transparent glass ceramics," J. Alloys Compd., 323-324 753-58 (2001).

[11]X. Qiao, Q. Luo, X. Fan, and M. Wang, "Local vibration around rare earth ions in alkaline earth fluorosilicate transparent glass and glass ceramics using Eu^{3+} probe," J. Rare Earths, 26[6] 883-88 (2008).

[12]W. Glass, J. Toulouse, and P. A. Tick, "Visible emission from rare earth ions in nanocrystal-containing glasses," J. Non-Cryst. Solids, 222 258-65 (1997).

[13]M. Sroda, C. Paluszkiewicz, M. Reben, and B. Handke, "Spectroscopic study of nanocrystallization of oxyfluoride glasses," J. Mol. Struct., 744-747 647-51 (2005).

[14]M. Sroda and Z. Olejniczak, "Effect of alkaline earth oxides on ceramization of LaF_3 in aluminosilicate glass: ^{19}F MAS-NMR study," J. Non-Cryst. Solids, 357[7] 1696-700 (2011).

[15]S. Xu, D. Deng, R. Bao, H. Ju, S. Zhao, H. Wang, and B. Wang, "Ni^{2+}-doped new silicate glass-ceramics for superbroadband optical amplification," J. Opt. Soc. Am. B, 25[9] 1548-52 (2008).

[16]R. Moncorge, J. Ther, D. Vivien, "Enhancement of fluorescence from octahedrally corrdinated Ni^{2+} in $LaMgAl_{11}O_{19}$ materials by Al^{3+}/Ga^{3+} ion substitution," J. Luminesc., 43 167-72 (1989).

[17]L. Galoisy, G. Calas, "Structural environment of nickel in silicate glass / melt systems: Part 1 Spectroscopic determination of coordination states," Geochim. Cosmochim. Acta, 57 3613-26 (1993).

[18]L. Galoisy, G. Calas, L. Cormier, B. Marcq, M.H. Thibault, "Overview of the environment of Ni in oxide glasses in relation to the glass colouration," Phys. Chem. Glasses, 46[4] 394-99 (2005).

[19]A. Dugué, L. Cormier, O. Dargaud, L. Galoisy, and G. Calas, "Evolution of the Ni^{2+} Environment During the Formation of a $MgO–Al_2O_3–SiO_2$ Glass-Ceramic: A

Combined XRD and Diffuse Reflectance Spectroscopy Approach," J. Am. Ceram. Soc., 95[11] 3483-89 (2012).

[20]W. W. Wendlandt and H. G. Hecht, "Reflectance spectroscopy." Wiley Interscience: New-York, (1966).

[21]A. Manceau, G. Calas, and A. Decarreau, "Nickel-bearing clay minerals; I, Optical spectroscopic study of nickel crystal chemistry," Clay Miner., 20[3] 367-87 (1985).

[22]G. R. Rossman, R. D. Shannon, and R. K. Waring, "Origin of the yellow color of complex nickel oxides," J. Solid St. Chem., 39[3] 277-87 (1981).

[23]B. Ravel and M. Newville, "ATHENA, ARTEMIS, HEPHAESTUS: data analysis for X-ray absorption spectroscopy using IFEFFIT," J. Synchrotron Radiat., 12[4] 537-41 (2005).

[24]M. Newville, "IFEFFIT : interactive XAFS analysis and FEFF fitting," J. Synchrotron Radiat., 8[2] 322-24 (2001).

[25]F. Farges, G.E. Jr. Brown, P.-E. Petit, M. Muñoz, "Transition elements in water-bearing silicate glasses/melts. Part I. A high-resolution and anharmonic analysis of Ni coordination environments in crystals, glasses, and melts," Geochim. Cosmochim. Acta, 65[10] 1665-78 (2001).

[26]E. M. A. Hamzawy and E. M. El-Meliegy, "Crystallization in the Na_2O-CaO-Al_2O_3-SiO_2-(LiF) glass compositions," Ceram. Int., 33[2] 227-31 (2007).

[27]N. Hémono, G. Pierre, F. Munoz, A. de Pablos-Martin, M. J. Pascual, and A. Duran, "Processing of transparent glass-ceramics by nanocrystallisation of LaF_3," J. Eur. Ceram. Soc., 29[14] 2915-20 (2009).

[28]S. Bhattacharyya, T. Höche, N. Hemono, M. J. Pascual, and P. A. van Aken, "Nano-crystallization in LaF_3-Na_2O-Al_2O_3-SiO_2 glass," J. Cryst. Growth, 311[18] 4350-55 (2009).

[29]L. Galoisy, L. Cormier, G. Calas, V. Briois, "Environment of Ni, Co and Zn in low alkali borate glasses: information from EXAFS and XANES spectra," J. Non-Cryst. Solids, 293-295 105-11 (2001).

[30]O. S. Dymshits, A. A. Zhilin, T. I. Chuvaeva, and M. P. Shepilov, "Structural states of Ni(II) in glasses and glass-ceramic materials of the lithium-aluminium-silicate system," J. Non-Cryst. Solids, 127 44-52 (1991).

[31]J. Petiau, G. Calas, Ph. Sainctavit, "Recent developments in the experimental studies of XANES," J. Phys. Colloq., 48 C9-1085-C9-96 (1987).

[32]L. Kido, M. Müller, and C. Rüssel, "High temperature vis-NIR transmission spectroscopy of iron-doped glasses," Phys. Chem. Glasses, 51[4] 208-12 (2010).

[33]G. Calas, O. Majérus, L. Galoisy, L. Cormier, "Crystal field spectroscopy of Cr^{3+} in glasses: compositional dependence and thermal site expansion," Chem. Geol., 229 218-26 (2006).

[34]A. de Pablos-Martin, A. Duran, and M. J. Pascual, "Nanocrystallisation in oxyfluoride systems: mechanisms of crystallisation and photonic properties," Int. Mater. Rev., 57[3] 165-86 (2012).

[35]T. J. Kiczenski, L.-S. Du, and J. F. Stebbins, "The effect of fictive temperature on the structure of E-glass: A high resolution, multinuclear NMR study," J. Non-Cryst. Solids, 351 3571-78 (2005).

[36]B. Cochain, L. Cormier, P. Florian, and Z. Zhang, (In preparation).

[37]L. Kukkonen, I. M. Reaney, D. Furniss, and A. B. Seddon, "Nucleation and crystallisation behaviour of transparent, erbium III doped, oxyfluoride glass ceramics for active photonic devices," Phys. Chem. Glasses, 42[3] 265-74 (2001).

[38]H. S. O'Neill, W. A. Dollase, and C. R. Ross, "Temperature dependence of the cation distribution in nickel aluminate ($NiAl_2O_4$) spinel - A powder XRD study," Phys. Chem. Miner., 18[5] 302-19 (1991).

[39]Y. S. Han, J. B. Li, X. S. Ning, and B. Chi, "Temperature Dependence of the Cation Distribution in Nickel Aluminate Spinel from Thermodynamics and X-Rays," J. Am. Ceram. Soc, 88[12] 3455-57 (2005).

Figure Captions

Fig. 1: Schematic representation of the insertion of the high temperature Linkam heating stage in the UV-Vis-NIR spectrometer.

Fig. 2: *In situ* X-ray diffraction patterns after background subtraction at the temperature indicated (°C) from room temperature up to 800°C. The most intense peaks are indentified by the Miller indices, the letter before the Miller indices represents the phase (L for LaF_3 crystals, N for nepheline and S for $NiAl_2O_4$ spinel).

Fig. 3: (a) *In situ* UV-Vis-NIR spectra for the parent glass and during heat-treatment at the indicated temperatures (700-780°C); (b) diffuse reflectance spectra of the final glass-ceramics products annealed for 120 minutes at the indicated temperatures (700-800°C) compared with the spectrum for $NiAl_2O_4$ spinel; (c) *in situ* UV-Vis-NIR spectra recorded isothermally at 750°C with the annealing time indicated (1-100 minutes).

Fig. 4: *In situ* XANES spectra at the Ni K-edge for the parent glass and during heat-treatment at the indicated temperatures (750-800°C) compared with the XANES spectrum for $NiAl_2O_4$ spinel.

Fig. 5: (a) *In situ* XANES pre-edge features for the parent glass and during heat-treatment at the indicated temperatures (700-850°C) and (b) and evolution upon temperature of the extracted pre-edge maximum intensity.

Figure 1

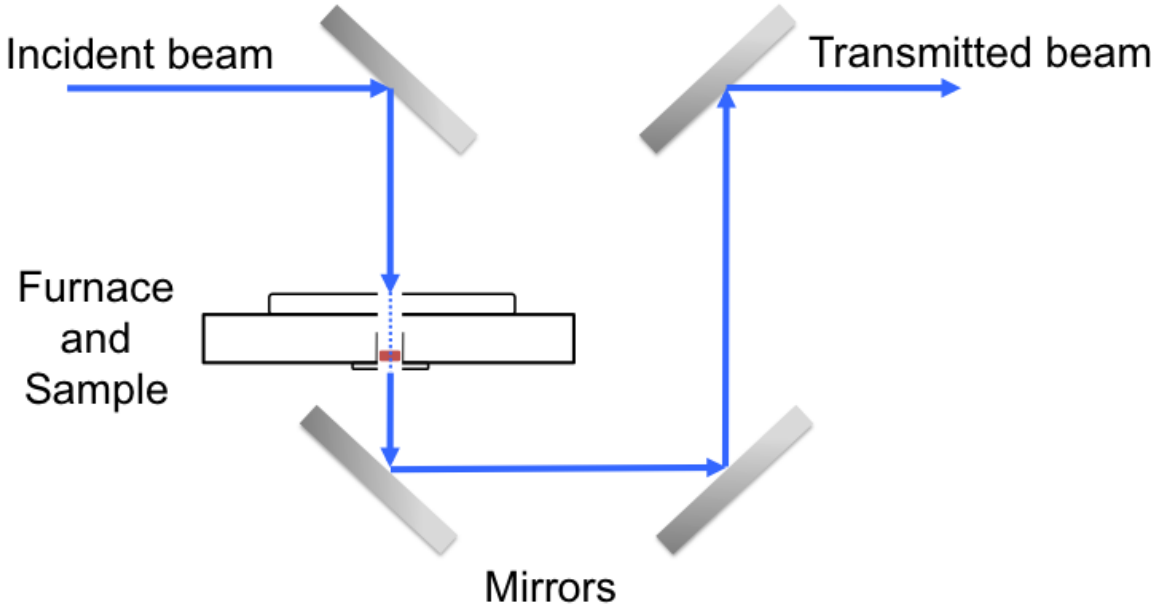
Incident beam
Transmitted beam
Furnace
and
Sample
Mirrors

Figure 2

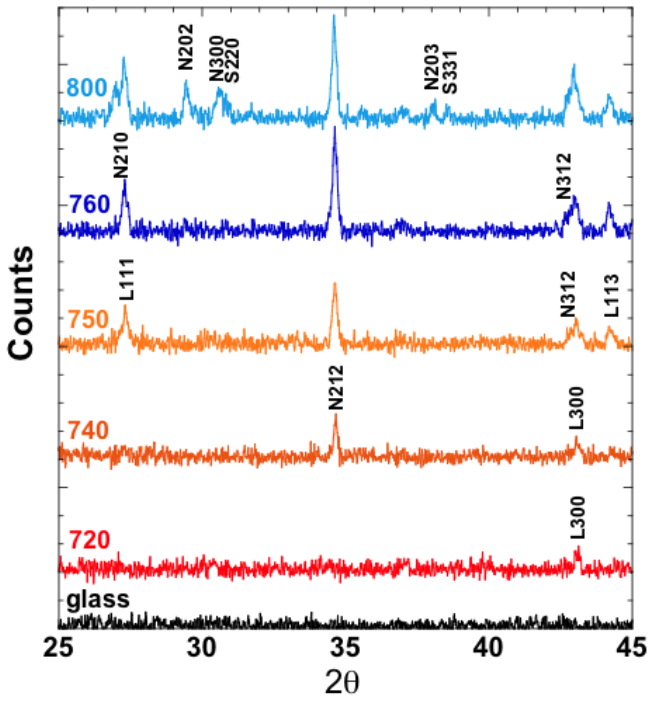
800
760
750
740
720
glass
N202
N300
S220
N203
S331
N210
N312
L111
N312
L113
N212
L300
L300
Counts
25
30
35
40
45
2θ

Figure 3

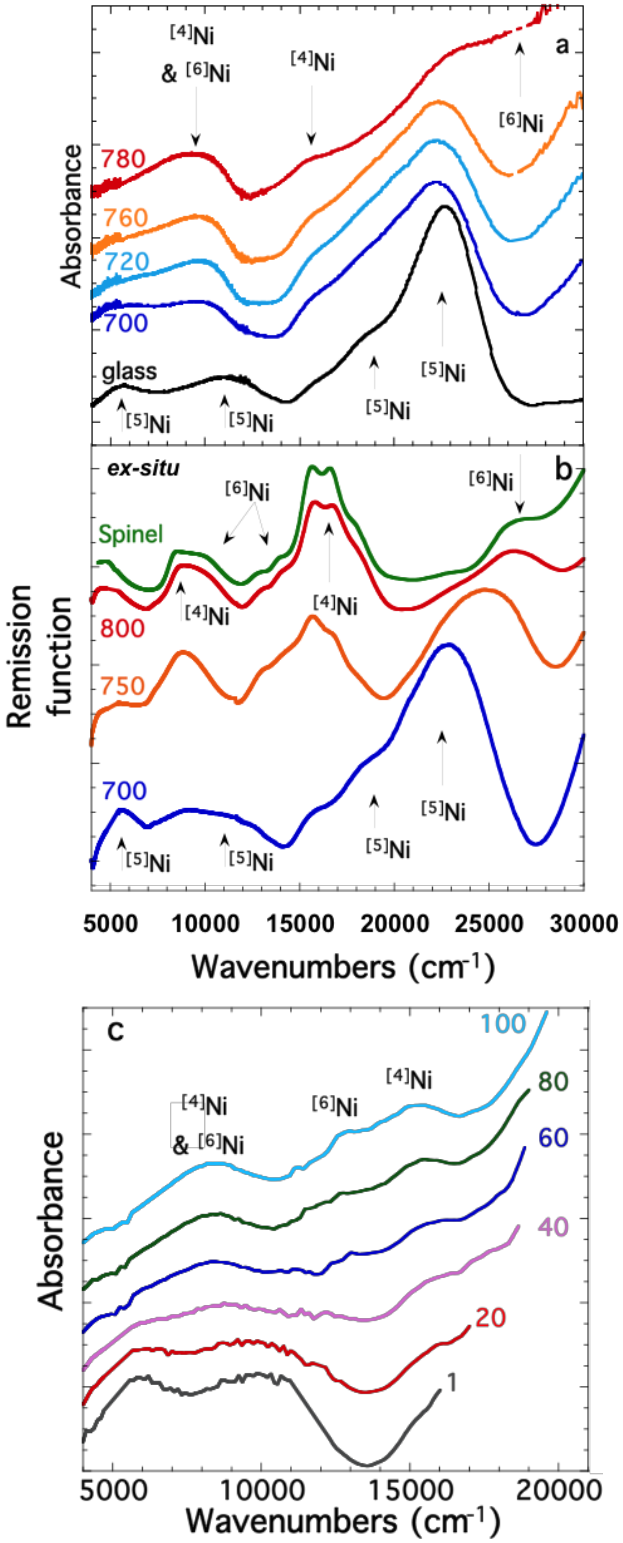
a
[4]Ni
& [6]Ni
[4]Ni
[6]Ni
780
760
720
700
glass
[5]Ni
[5]Ni
[5]Ni
[5]Ni
Absorbance
b
ex-situ
[6]Ni
[6]Ni
Spinel
[4]Ni
[4]Ni
800
750
700
[5]Ni
[5]Ni
[5]Ni
[5]Ni
Remission function
5000
10000
15000
20000
25000
30000
Wavenumbers (cm-1)
c
100
80
60
40
20
1
[4]Ni
& [6]Ni
[6]Ni
[4]Ni
Absorbance
5000
10000
15000
20000
Wavenumbers (cm-1)

Figure 4

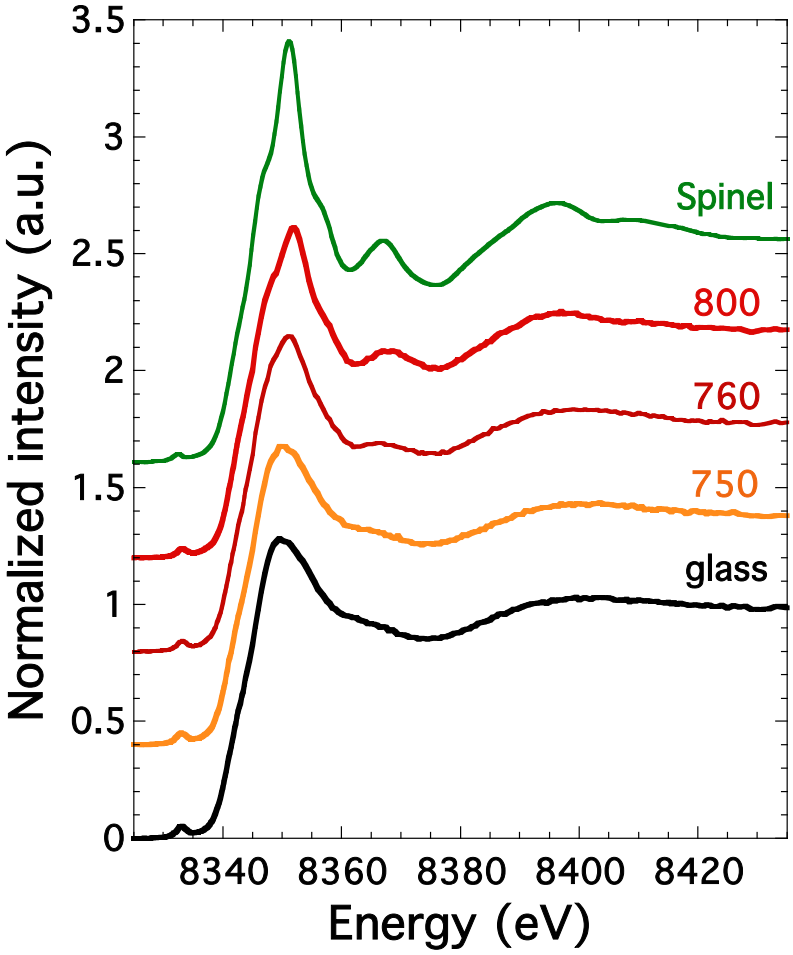
Normalized intensity (a.u.)
Energy (eV)
Spinel
800
760
750
glass
0
0.5
1
1.5
2
2.5
3
3.5
8340
8360
8380
8400
8420

Figure 5

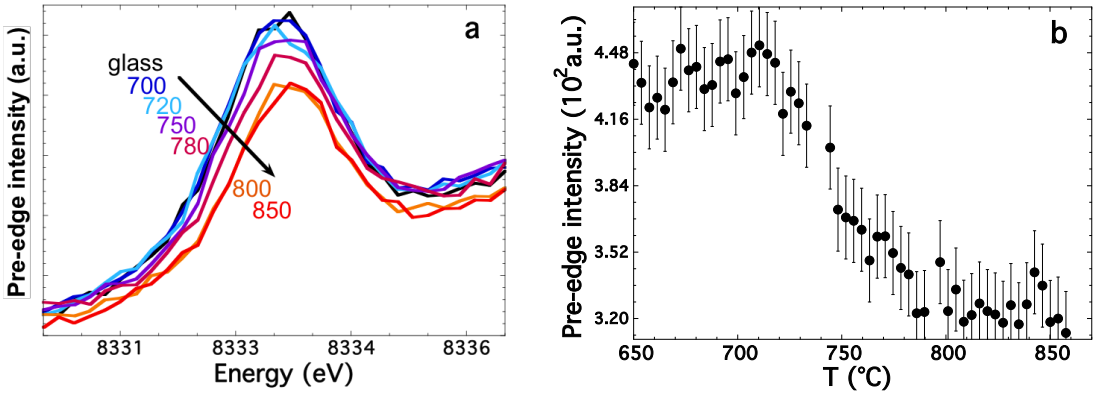
a
glass
700
720
750
780
800
850
Pre-edge intensity (a.u.)
8331
8333
8334
8336
Energy (eV)
b
Pre-edge intensity (10^2a.u.)
4.48
4.16
3.84
3.52
3.20
650
700
750
800
850
T (°C)